XMCD at the $L_{II,III}$ edges of Er in $ErMn_2$, $ErFe_2$, $ErCo_2$, $ErNi_2$, and $ErAl_2$ Laves phases and in $Er_2(SO_4)_3$, $8H_20$

Christine Giorgetti and Elisabeth Dartyge
Laboratoire pour l'Utilisation du Rayonnement Electromagnétique (LURE), Laboratoire CNRS-CEA-Ministère de la Jeunesse, de l'Education Nationale et de la Recherche, Bâtiment 209 D, Université Paris–Sud, Boîte Postale 34, 91898 Orsay CEDEX, France

François Baudelet
L.P.M.C., Tour 13, 4 place Jussieu, 75252 Paris CEDEX 05, France and LURE, Bâtiment 209 D, Université Paris–Sud, Boîte Postale 34, 91898 Orsay CEDEX, France

Rose-Marie Galéra
Laboratoire Louis Néel, CNRS, 25 avenue des Martyrs, Boîte Postale 166 X, 38042 Grenoble CEDEX 9, France
(Received 30 April 2003; revised manuscript received 26 March 2004; published 14 July 2004)

X-ray magnetic circular dichroism (XMCD) measurements have been performed at the $L_{II,III}$ edges of Er in the intermetallic compounds $ErMn_2$, $ErFe_2$, $ErCo_2$, $ErNi_2$, and $ErAl_2$, as well as in the ionic compound $Er_2(SO_4)_3, 8H_20$, in order to study the evolution of the XMCD spectra as a function of the 5*d* states filling and/or their hybridization with magnetic or nonmagnetic electronic states. Almost all the spectra present the same general features, confirming that the 4*f*-5*d* intra-atomic coupling is a key point to explain XMCD spectra. Thus, we analyze the models based on this interaction, proposed to account for the unexpected sign of *E*1 -XMCD measurements, as well as the nonstatistical branching ratio between XMCD at the L_{II} and L_{III} edges. We underline the impossibilities of reproducing our measurements using these models. Moreover, we point out the special role played by Fe which leads, at the L_{II} edge of Er, to a significant modification of the shape of XMCD spectrum and an unexpected temperature dependence. The XMCD revealed an unexpected behavior of the 5*d* magnetic polarization in these compounds which is not visible in macroscopic measurements. This also demonstrates the non-negligible role played by the 5*d*-3*d* hybridization.

DOI: 10.1103/PhysRevB.70.035105 PACS number(s): 78.70.Dm, 71.20.Eh, 71.20.Lp, 78.20.Ls

I. INTRODUCTION

X-ray magnetic circular dichroism (XMCD) is the difference between absorption cross sections of left- and right handed circularly polarized x rays, which is observed in magnetic systems presenting a net magnetization.[1] Except in coercitive ferro- or ferrimagnetic systems, where a remnant magnetization remains in zero field, an applied magnetic field is required to induce the net magnetization in all the other systems. XMCD can then be observed in ferromagnetic, ferrimagnetic, and paramagnetic systems as soon as the applied field is intense enough to induce this net magnetization. Due to the spin-orbit coupling in the initial or final states of the photoinduced transition, the orbital selection rules of the dipolar electric (*E*1) Hamiltonian are transferred to the spin properties. Thus, taking benefits of the selectivity of x-ray absorption, the XMCD should be a powerful tool to study the magnetic polarization of each electronic shell of each atomic species in complex materials. Using the sum rules,[2–5] one should be able to deduce the orbital and spin moments of the probed shell.

In metallic rare-earth (RE) based materials, the RE 5*d* states, though they barely contribute to the local magnetic moment, play an important role: the strongly localized character of 4*f* states prevents the overlapping between these states and the other atoms of the material. The 5*d* states of the RE, whose polarization is induced by the 4*f*-5*d* intra-atomic coupling, are band states and are considered to mediate the magnetic interactions through the crystal. For instance, in the rare-earth–transition-metal (RE-TM) intermetallics, where the TM is a heavy 3*d* metal, the hybridization of the 5*d* and 3*d* bands leads to an antiferromagnetic coupling between the 5*d* and 3*d* spins. This originates the ferromagnetic and antiferromagnetic behavior in the light RE and heavy RE compounds respectively.[6] The possibility of probing directly the 5*d* state polarization using the XMCD at the $L_{II,III}$ edges of RE($E1{:}2p_{1/2,3/2} \rightarrow 5d_{3/2,5/2}$) is thus of interest to get a deeper insight into the fundamental mechanism of magnetic interactions. An extensive series of experiments at the $L_{II,III}$ edges of RE have been done on these systems,[7–12] whose interpretation is still a matter of debate. Even if most of the studies have been carried out on RE-TM intermetallic compounds, the points summarized below are not specific to these systems but are also observed in pure metallic RE compounds and in ionic RE compounds.

One of the difficulties was the presence of quadrupolar electric transitions ($E2{:}2p_{1/2,3/2} \rightarrow 4f_{5/2,7/2}$).[13] They were not taken into account in the first analyses.[14,15,8,9] The *E*2 transitions appear just below the *E*1 transitions. Their contribution to the spectra is now doubtless,[16–21] even if their experimental evidence is difficult to achieve at the L_{II} edge.[21,22]

Another difficulty comes from the sign of the *E*1 contribution. From the early one-particle model of Schütz *et al.*,[1] the XMCD should be directly proportional to the product of

the Fano factor,[23] which defines the rate of spin-polarization of photoelectrons, by the spin polarization rate of the empty states. It was then expected to deduce the sign of the projection of the 5*d* spin polarization on the quantization axis $\langle S_z(5d)\rangle$ directly from the sign of XMCD measurements. This model has been successfully applied to 5*d* transition metals like Hf, Lu,[9–11,24–26] or La,[27] and also in mixed valence cerium.[10,11] This sign can also be drawn from the so-called spin sum rule[4] in neglecting the magnetic dipole operator term $\langle T_z\rangle$. *In the case of RE systems, as soon as the 4f shell is partially filled and localized, the sign of* $\langle S_z(5d)\rangle$ *deduced from XMCD measurements is opposite to the one resulting from magnetic interactions*.[9] To solve this inconsistency, a different radial overlap between the 2*p* core hole and the up and down 5*d* subbands[18] has been invoked, based on a spin-polarized band-structure calculation in metallic Gd showing that the 5*d* spin subbands had different radial extension.[28] The results obtained in $RE(Ni_xCo_{1-x})_5$ compounds (RE = La, Gd, and Tb) at the L_{III} edge of RE can apparently support this model.[27]

In addition to the reversal of the sign observed for RE with an open and localized 4*f* shell, the ratio of XMCD effects at the L_{II} and L_{III} edges, labeled $\Re(L_{II}/L_{III})$, has got, in most of the cases, nothing to do with the statistical value[9] derived from the model proposed by Schütz *et al.*[1] Since this model implies no orbital momentum in the 5*d* band, i.e., no difference between the $5d_{3/2}$ and $5d_{5/2}$ subbands, the spin-polarization rate of the empty states probed at the L_{II} and L_{III} edges should be the same. Thus the value of the statistical branching ratio is given by the ratio between the Fano factors at the L_{II} and L_{III} edges, respectively, and is evaluated to −2 by atomic calculation. This statistical value is observed for 5*d* transition metals.[9–11,24–27] A deviation to the statistical value of $\Re(L_{II}/L_{III})$ should imply the presence of an orbital momentum in the probed band. The same conclusion can be drawn from the application of the so-called orbital sum rule.[2,3] Of course, the fact that the sign of $\langle S_z\rangle$, predicted by the concerning sum rule[4] (neglecting the $\langle T_z\rangle$ term) is wrong, should make us cautious with the application of the sum rules to such measurements. In a preceding paper, we showed that the ratio of XMCD effects at the L_{II} and L_{III} edges was proportional to $\langle L_z(4f)\rangle$.[9] The result of this previous paper has to be reconsidered today because it was concluded at a moment where the *E*2 transitions were not evidenced, so they were integrated in the *E*1 contribution. Moreover, most of the measurements of that previous study were done on Fe compounds and, as it will be shown in this present paper, the compound with Fe presents specific features mostly at the L_{II} edge. The conclusion that the non-statistical value of $\Re(L_{II}/L_{III})$ could be linked to $\langle L_z(4f)\rangle$ can still be drawn by considering only the *E*1 contribution. Indeed, the statistical value of the ratio [observed for La in $LaCo_5$ (Ref. 27) and Lu in $LuFe_2$ (Ref. 9)] is also observed for Gd in $GdFe_2$,[11,12] Gd_2Fe_{17},[11] Gd_2Co_{17},[8] and $GdNi_5$.[27] In Gd, there is no 4*f* orbital momentum. For the light RE, such as Nd in Nd_2Fe_{17} (Refs. 11 and 12) and Pr in Pr_2Co_{17},[8,11,12] the XMCD signal at the RE L_{III} edge is much smaller than the one at the L_{II} edge; for heavy RE the XMCD signal at the L_{II} edge is smaller than the one at the L_{III} edge [for instance, the ratio is equal to −1 instead of −2 for Tb in $TbFe_2$,[11,12] Tb_2Co_{17} [8] and $TbNi_5$ (Ref. 27)]. This variation was at the origin of the idea that the orbital momentum of the 5*d* band may be induced by the 4*f* orbital momentum.

To explain both the sign and the branching ratio of *E*1 XMCD signals at the L_{II} and L_{III} edges of RE, models generalizing the spin dependence of the radial part of the matrix elements of Gd have been proposed: they are based on an enhancement of the matrix elements (EME) resulting from the spin and orbital 4*f*-5*d* Coulomb exchange interaction. The two main ones have been developed by van Veenendaal *et al.*[29,30] and Matsuyama *et al.*[31–33]

Since the XMCD at the $L_{II,III}$ edges of RE probes hybridized band states, it is also important to evaluate the influence of the surroundings of the RE on the XMCD signal. To study this effect, we have carried out measurements at the $L_{II,III}$ edges of one typical RE, Er, in systems where Er is alloyed with a nonmagnetic metal: $ErAl_2$, or with different 3*d* metals: $ErMn_2$, $ErFe_2$, $ErCo_2$, and $ErNi_2$. These compounds are Laves phases with almost the same local crystallographic symmetries, to prevent the superimposition of effects that should arise from the modification of this parameter. The change of the alloyed metal allows one to test the influence of (i) the 5*d*-3*p* or 5*d*-3*p* hybridization, and (ii) the 3*d* metal magnetic state. For comparison purposes, we also study $Er_2(SO_4)_3$, $8H_20$, where Er is in the ionic state Er^{3+} and the 5*d* states are considered to be empty.

Our study allows us to investigate a different parameter than the ones explored by the other systematic studies done at the $L_{II,III}$ edges of RE.[34,35] Neumann *et al.*[34] studied the $L_{II,III}$ edges of different RE in ionic systems. This study served as a basis for the model developed by van Veenendaal *et al.*[29,30] Fukui *et al.*[35] studied the XMCD at the $L_{II,III}$ edges of all the RE in the $RE_2Fe_{14}B$ series; this study was analyzed in a framework deriving from the model proposed by Matsuyama *et al.*[31]

In light of our experimental results, we analyze, discuss, and apply the models, which take into account the enhanced matrix elements to explain the sign and the branching ratio of the XMCD signals. Our results are also compared to other experimental works. The paper is divided as follows. In Sec. II we give experimental details. Experimental results are described and discussed in Sec. III. Section IV, devoted to the analysis and the discussion of models, is separated into three parts. In Secs. IV A and IV B, we analyze the proposed models, apply them to our measurements, and compare our results with those obtained by Neumann *et al.*[34] and Fukui *et al.*[35] Finally, in Sec. IV C, we summarize the evolution of ideas which led to the proposed models and we discuss their consequences on the sum rules. In Sec. V, we conclude our experimental results and our application of the models by outlining their differences, what they are able to reproduce, and what still failed, according to our results.

II. SAMPLES, EXPERIMENTAL DETAILS, CONVENTIONS, AND DATA TREATMENT

For this study, binary compounds of metallic RE with a magnetic or a nonmagnetic metal have been chosen. As

TABLE I. Curie temperature, magnetization at saturation, and experimental conditions (temperature and magnetic field) of XMCD measurements.

	$ErMn_2$	$ErFe_2$	$ErCo_2$	$ErNi_2$	$ErAl_2$	$Er_2(SO_4)_3,8H_20$
T_c (K)	22	587	38.8	7	12	none
$M_{sat}(\mu_B)$ at 10 K		4.84	5.62	para	7.06	para
$T_{measurement}$ (K)	14	10	10	14	10	10
$B_{measurement}$ (T)	1.8	1.8	1.8	1.8	1.45	1.8

model systems, these compounds have attracted a great interest for more than four decades since they allow one to study fundamental problems in magnetism. For instance, the RE Al_2 has been well suited to validate the crystal electric field framework for RE solids,[36] while the RE-3*d* metal compounds are illustrative of the conditions of the onset of the 3*d* magnetism.[37] The $ErTM_2$ with TM=Al, Fe, Co, and Ni crystallize in the cubic $MgCu_2$ Laves phase structure (C15, space group F*d*-3*m*) with Er at the 8*a* site and TM at the 16*d* site. $ErMn_2$ crystallizes in the hexagonal $MgZn_2$ Laves phase structure (C14, space group *P*63/mmc) with Er at the site 4*f* and Mn at the sites 2*a* and 6*h*. Actually, the local electronic and crystallographic environments of the Er site in the C14 and C15 structures are not very different. In $ErMn_2$ and $ErNi_2$, the 3*d* metal bears no magnetic moment. In $ErCo_2$, the Co moment is induced by the magnetic rare earth while in $ErFe_2$, the Fe satisfies the Stoner criterion and the strong Fe-Fe interactions are responsible for the high Curie temperature T_C=587 K and the existence of a temperature of compensation T_{comp}=486 K. In $ErAl_2$, polarized neutron studies have revealed the absence of polarization for the conduction electrons or 5*d* electrons, contrary to the other intermetallic compounds of the series.[38]

The sulphate compound $Er_2(SO_4)_3,8H_20$ belongs to the monoclinic system. Er is in the ionic state Er^{3+}, the 5*d* orbitals are supposed to be empty and well localized; its magnetization follows a Brillouin function.

The bulk polycrystalline intermetallic compounds were prepared at the Laboratoire de Magnétisme Louis-Néel, by radio frequency melting under argon pressure in a cold copper crucible from the stoichiometric proportions of 99.99% pure elements. As these compounds do not all melt congruently, the crystallographic phase of the ingots was checked by x-ray diffraction using the Debye-Scherrer geometry. All the diffraction patterns are in agreement with the C14 and C15 structures. The amount of impurities or other phases is less than 5%, as their presence cannot be detected in the patterns. For all the samples, part of the ingot was spark cut in order to carry out the magnetic measurements. Magnetization curves were recorded using an extraction method in fields up to 8 T, supplied by a cryomagnet in the temperature range of 1.5–300 K. The magnetization at saturation and the Curie temperature are deduced from the Arrott plots (M^2 as a function of $\mu_0 H/M$). For all the compounds these two quantities are in agreement with the values previously reported[36,37] (see Table I).

For XMCD measurements, the rest of the ingots was crushed into powder in a cyclohexane solution to avoid oxidation, layered onto a polycarbonate membrane, pasted with nitrocellulose solution of collodion, and covered with a Kapton scotch film.

The XMCD measurements were carried out on the energy dispersive x-ray absorption beamline of the positron-injected storage ring DCI at the French synchrotron radiation facility LURE in Orsay. This setup[39] allows absorption measurements in transmission geometry. The polychromator was a Si(111) crystal, curved to achieve a focus point at 1.2 m away, where the samples are placed. The position sensitive detector is an array of 1024 Si photodiodes. With such a spectrometer, the energy resolution is better than 2 eV.[40] Harmonics were rejected using a SiO_2 mirror positioned between the sample and the detector. Right circularly polarized photons (polarization rate of about 50%[41]) were selected by positioning a 1 mm wide slit at 0.23 mrad below the synchrotron orbit plane. The net magnetization of the sample, required to observe a XMCD signal, is induced with an electromagnet supplying a field up to 1.8 T, positioned along the propagation of photons around the focus point. An XMCD signal is obtained from the difference of successive x-ray absorption spectra recorded with the applied magnetic field parallel and antiparallel to the photon propagation vector.

The sign of our XMCD spectra is defined as follows: XMCD spectra are the difference of absorption cross sections measured by using right-handed circularly polarized photons (σ^-), with magnetic field parallel ($+B$), then antiparallel ($-B$) to the wave vector of the incident beam. The XMCD spectra are then proportional to $[\sigma^-(+B)-\sigma^-(-B)]$ $=[\sigma^-(+B)-\sigma^+(+B)]$. By considering as a reference the magnetic field parallel to the wave vector of photons, XMCD is proportional to $(\sigma^- - \sigma^+)$. For historical reasons, this convention is adopted by all the experimentalists.

The samples were cooled down using a cryocompressor. The values of the temperature and the magnetic field of XMCD measurements are sketched in Table I. Under these temperature conditions, the $ErMn_2$, $ErFe_2$, $ErCo_2$, and $ErAl_2$ samples were in the ferromagnetic state, while $ErNi_2$ and $Er_2(SO_4)_3,8H_20$ were in the paramagnetic state. The temperature dependence of XMCD spectra has been studied on $ErFe_2$ and $ErCo_2$ samples. In the six systems, and for all the temperatures, the magnetization of Er is parallel to the external magnetic field giving the quantization axis. The total angular momentum J_{4f}, the orbital angular momentum L_{4f}, and the spin S_{4f} align antiparallel to the quantization axis. Due to the positive intra-atomic exchange, the spin of 5*d* electrons S_{5d} aligns parallel to S_{4f}, i.e., antiparallel to the quantization axis. (The hybridization between 5*d* and 3*d* spins leading to an antiparallel coupling, S_{3d}, aligns parallel to the quantization axis and the 3*d* magnetic moment is finally antiparallel

to the magnetic moment carried by Er. This scheme is in agreement with the well-known ferrimagnetic coupling between the heavy RE and the 3*d* TM.[6])

After subtraction of the background, the absorption spectra are normalized to 1 (point taken at about 300 eV above the edge corresponding to transitions to the continuum). This constant scaling factor is the so-called jump edge. The XMCD spectra are divided by the jump edge at the L_{II} and L_{III} edges. Because the absorption cross section at the L_{II} edge is twice as small as at the L_{III} edge, the XMCD at the L_{II} edge is artificially multiplied by 2, as compared to the XMCD at the L_{III} edge. For this reason, the values of XMCD signals at the L_{II} edge presented in this paper must be multiplied by $1/2$ when reported in theoretical expressions.

To allow the comparison between the L_{II} and L_{III} edges, the spectra are sometimes plotted versus the relative energy E-E_0, where the energy of the edge E_0 is conventionally taken at the inflexion point of the absorption spectrum.

III. EXPERIMENTAL RESULTS AND DISCUSSION

In Fig. 1 are presented the absorption spectra at the L_{III} [Fig. 1(a)] and L_{II} [Fig. 1(b)] edges of Er in $Er_2(SO_4)_3$, $8H_20$, $ErAl_2$, $ErMn_2$, $ErFe_2$, and $ErCo_2$. The x-ray absorption near edge structure (XANES) (oscillations in the absorption spectra to around 50 eV above the edge) and the extended x-ray absorption fine structure (EXAFS) (following oscillations) are representative of the local electronic and crystallographic structures, respectively. The XANES as well as the EXAFS at the $L_{II,III}$ edges of Er in $ErMn_2$ are the same as in $ErFe_2$ and $ErCo_2$ (and $ErNi_2$—not shown for the sake of clarity), which confirms that the local electronic and crystallographic environments of the RE are not modified between the C14 and the C15 Laves phase structures. The thin and intense white line in $Er_2(SO_4)_3$, $8H_20$ is characteristic of a peak of empty and localized 5*d* density of states, confirming the ionic character of Er in the sulphate compound. In the other systems, the metallic character is shown by the wider and less intense white line, in agreement with a 5*d* band widened by strong hybridization. This effect is more pronounced in the metallic systems with 3*d*-5*d* hybridization (Mn, Fe, Co, and also Ni) than in the compound with A1. Another consequence of the hybridization in the metallic systems is the charge transfer into the 5*d* band, leading to the screening of the Coulomb interaction due to the 2*p* core hole: the *E*1 transitions arise at lower energy in the metallic compounds as compared to the ionic one. The observed shift is around 2.5 ± 0.5 ev for both edges, with $E_0(L_{III})=8358$ eV and $E_0(L_{II})=9264$ eV for the metallic systems.

The XMCD signals at the $L_{II,III}$ edges of Er in $Er_2(SO_4)_3$, $8H_20$, $ErAl_2$, $ErMn_2$, $ErFe_2$, $ErCo_2$, and $ErNi_2$ are shown in Fig. 2. One observes that the XMCD spectra at the L_{III} edge (Fig. 2, left-hand side) have the same shape and sign in the six compounds. With the convention previously defined, the first peak at low energy (below 8357 eV) is negative and can be attributed to *E*2 transitions.[13,18,19,21] The second one at higher energy (above 8357 eV), is positive and is considered to be of *E*1 origin. The *E*1-XMCD spectrum of the sulfate compound is more structured: it exhibits a small negative

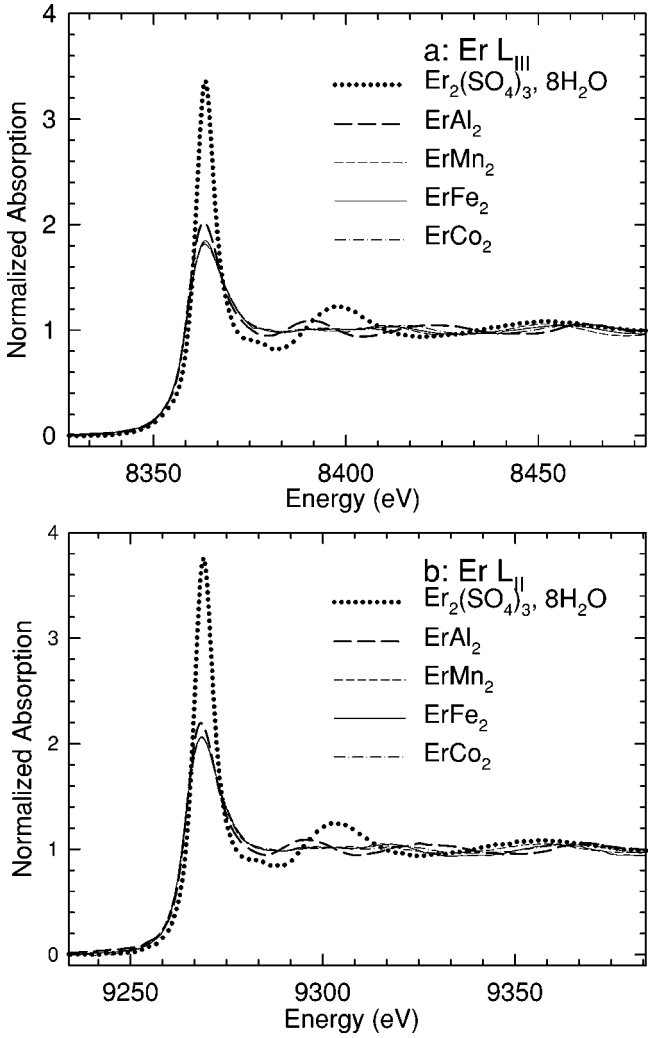

FIG. 1. Absorption spectra at (a) the L_{III} edge and (b) the L_{II} edge of Er in $Er_2(SO_4)_3$, $8H_20$, $ErAl_2$, $ErMn_2$, $ErFe_2$, and $ErCo_2$.

structure at 10 eV. The small negative-positive feature observed just before the edge in the $ErNi_2$ spectrum is a part of the XMCD at the *K* edge of Ni (8333 eV), which is 25 eV below the L_{III} edge of Er.

The width of the *E*1 peak at the L_{III} edge has the same behavior as the width of the absorption edge. It is more or less the same in $ErFe_2$, $ErCo_2$, and $ErNi_2$. It is narrower for $ErAl_2$, and again narrower in the ionic compound $Er_2(SO_4)_3$, $8H_20$. Due to this smaller width in $Er_2(SO_4)_3$, $8H_20$, the separation between the *E*1 and *E*2 contributions is more pronounced, which allows one to evaluate the energy of the maximum of the *E*2 structure at 8353.5 ± 0.5 eV (-7 eV below the ionic edge). The maximum of the *E*2 contribution at the L_{III} edge for the metallic compounds also points to the same energy. This means that the overlap between *E*1 and *E*2 contributions in the metallic compounds is not very important, and is in agreement with the fact that the 4*f* states are well localized inside the atom, thus less sensitive to the surroundings.

At the L_{II} edge (Fig. 2, right-hand side), XMCD signals present the same shape for all the compounds under study, except $ErFe_2$. In $ErMn_2$, $ErCo_2$, $ErNi_2$, $ErAl_2$, and $Er_2(SO_4)_3$,

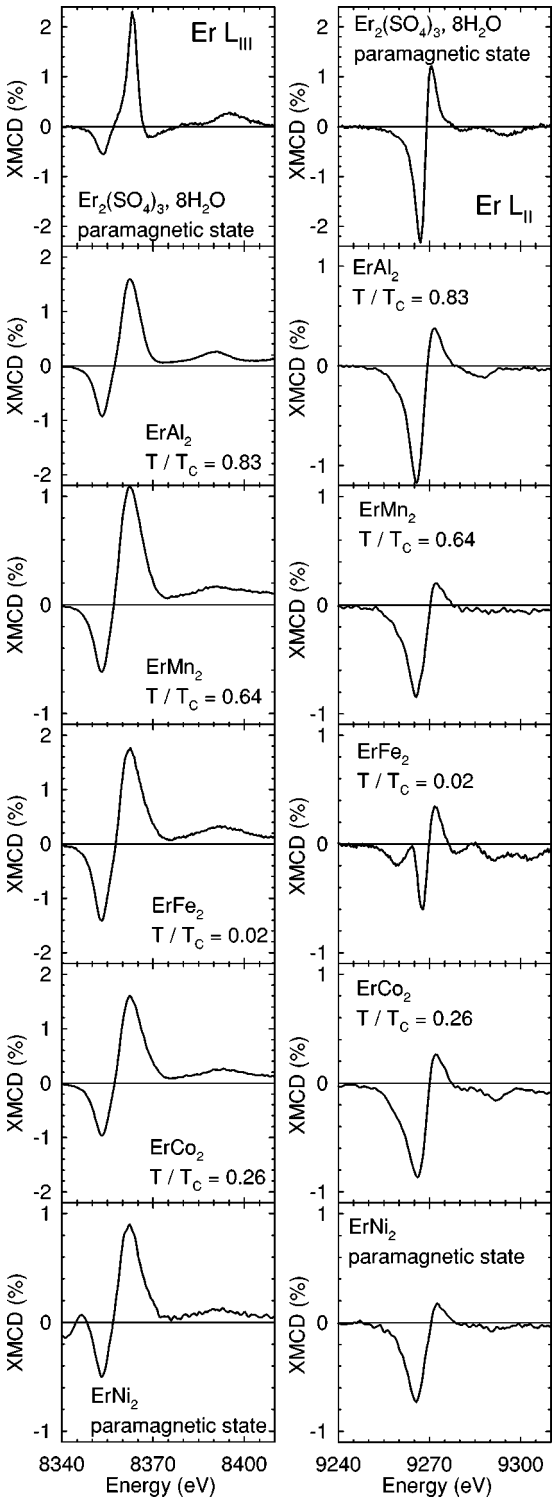

FIG. 2. XMCD spectra at the L_{III} edge (left panel) and the L_{II} edge (right panel) of Er in $Er_2(SO_4)_3$, $8H_20$, $ErAl_2$, $ErMn_2$, $ErFe_2$, $ErCo_2$, and $ErNi_2$.

$8H_20$, the XMCD signals are constituted of one main negative peak between 9247 and 9269 eV, followed by a small positive one between 9269 and 9269 eV The angular variation of the two peaks of the XMCD signal at the Er-L_{II} edge in $ErCo_2$ and $ErAl_2$ follows, within the precision of the measurements, a cosine law characteristic of $E1$

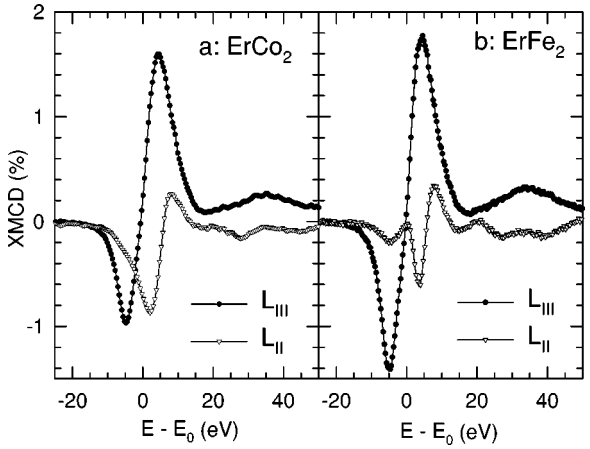

FIG. 3. Superposition of XMCD spectra at the L_{II} and L_{III} edges of Er in (a) $ErCo_2$ and in (b) $ErFe_2$.

transitions.[42] In $ErFe_2$, the XMCD at the Er-L_{II} edge has a very structured shape: it is composed of one negative peak between 9269 and 9264 eV, whose angular variation was shown to be characteristic of $E2$ transitions,[21] followed by a quite thin derivative structure between 9264 and 9276 eV, of $E1$ origin.

At the L_{II} edge, the positive $E1$ peak of spectra (between 9269 and 9276 eV) in $ErMn_2$, $ErCo_2$, $ErNi_2$, and $ErAl_2$ coincides with the positive one of the derivative $E1$ structure of $ErFe_2$. The width of the negative structure is larger in all the compounds as compared to $ErFe_2$: it envelops both the $E2$ transitions and the negative part of the $E1$ transitions in the $ErFe_2$ spectrum. Another consequence of this larger width is that the negative part of the $E1$ signal at the L_{II} edge in $ErCo_2$ [or $ErMn_2$, $ErNi_2$, $ErAl_2$, and $Er_2(SO_4)_3$, $8H_20$] extends to the lower energies as compared to the L_{III} edge [Fig. 3(a)], while in $ErFe_2$, the derivative shape in XMCD at the L_{II} edge of Er inserts exactly in the positive peak of the spectrum at the L_{III} edge: the $E2$ and $E1$ contributions have exactly the same energy extension [Fig. 3(b)], from one edge to the other.

Apart from the $ErFe_2$ compound, where the two opposite peaks of $E1$ origin have more or less the same amplitude, the integrated $E1$-XMCD signal at the L_{II} edge is unambiguously negative. At the L_{III} edge, it is positive. A rough application of the spin sum rule[4] allows one to conclude that $\langle S_z(5d)\rangle$ extracted from XMCD measurements (when neglecting the $\langle T_z\rangle$ term) is always opposite to the expected one. Finally, one observes that the effect of dichroism at the L_{II} edge is smaller than at the L_{III} edge. Whatever the compound is, $E1$-XMCD(L_{II}) is never equal to twice $E1$-XMCD(L_{III}) as it should be with the adopted normalization convention.

When Fe is replaced by a $3d$ transition metal which does not satisfy the Stoner criterion, like Co, Ni, or Mn, the small negative part of $E1$ widens and increases; the shape of the signal is closer to the one of $ErAl_2$, where A1 is a $3p$ metal, and to the one of the ionic compound, $Er_2(SO_4)_3$, $8H_20$. The shape of the XMCD signal at the L_{II} edge of Er in $ErFe_2$ is characteristic of the XMCD signal measured at the L_{II} edge of heavy RE (Dy, Ho, Er, Tm) in RE Fe_2 compounds. In $TbFe_2$, the negative peak is quite large and one clearly sees

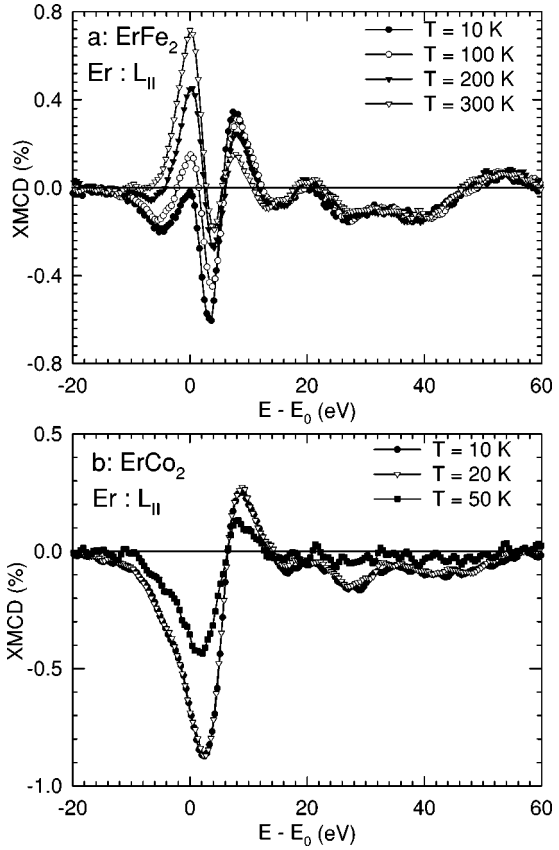

FIG. 4. Temperature dependence of XMCD at the L_{II} edge of Er in (a) $ErFe_2$ and (b) $ErCo_2$.

its narrowing when the RE becomes heavier.[11,12] The narrowness of the $E1$ XMCD signal at the L_{II} edge in $ErFe_2$, seems to be a characteristic of Laves phases with Fe. It cannot be simply explained by the fact that the number of $3d$ electrons decreases from Co to Fe, because the signal measured in $ErMn_2$ has the same shape as in $ErCo_2$.

We also measured the temperature dependence of the XMCD at both edges of Er in $ErFe_2$ and at the L_{II} edge in $ErCo_2$. When increasing the temperature, one observes at the Er-L_{II} edge in $ErFe_2$ [Fig. 4(a)][43] the emergence of a new positive peak at 0 eV, which overlaps the $E2$ contribution (-17 to 0 eV), with a simultaneous decrease of the negative part of the $E1$ signal (0 to 5 eV). The positive part of the $E1$ signal (5 to 12 eV) also decreases, but in the whole magnetic XANES (12 to around 50 eV) and EXAFS (above 50 eV) regions, the amplitude remains constant, as expected in ferromagnetic compounds. One emphasizes the fact that the range of temperatures explored (10–300 K) is far below the Curie temperature (587 K), and even the compensation temperature (496 K). No significant change in the $5d$ band is expected in this temperature interval. The decrease of the $E1$ structure at the Er-L_{II} edge in the $ErFe_2$ compound with increasing temperature cannot be explained by a normal decrease of the magnetization with temperature. This conclusion is reinforced by the thermal evolution of the signal at the Er-L_{II} edge in the $ErCo_2$ compound [Fig. 4(b)], where the amplitude of the signal is constant between 10 and 20 K(T_C=38.8 K) and decreases at the edge but also in the XANES region, with no change of shape at 50 K. Very surprisingly, at the Er-L_{III} edge of $ErFe_2$ (not presented), the thermal evolution of the XMCD signal does not present any change of shape and amplitude decrease.

A similar variation has also been observed in XMCD measurements at the L_{II} edge of Er in the deuteride $ErFe_2D_{3.4}$,[44] but in a temperature range above the compensation temperature, where the magnetic moment of Fe is dominant as compared to the one of Er. This confirms the idea that this effect is due to the influence of Fe.

To explain the specific behavior of heavy-RE-Fe_2 compounds as compared to Laves phases with other TM (the shape of XMCD at the RE-L_{II} edge and temperature dependence), one could think to magnetostriction, this effect being more important in the case of Fe systems. In these compounds, the magnetostrictive effect induces a rhombohedral distortion of the RE site,[45] which is also a consequence of the introduction of D in $ErFe_2$, since the $ErFe_2D_{3.4}$ compound is rhombohedral; the thermal evolution of the XMCD spectra should be a consequence of the temperature dependence of the magnetostriction. Nevertheless, the shape of the XMCD signal at the Er-L_{II} edge in $ErFe_2D_{3.4}$ is the same as that in $ErCo_2$. A wide and large negative peak is also observed at the Tb-L_{II} edge in $TbFe_2$ (Refs. 11,12) where the magnetostrictive effect is even more intense.[44] So the magnetostrictive effect is probably not at the origin of the particular shape of the XMCD signal at the Er-L_{II} edge in $ErFe_2$. Another important point is that the magnetic EXAFS does not change with temperature. The surprising behavior of the XMCD spectra at the L_{II} edge of Er with temperature is probably due to an evolution of the electronic structure rather than of the crystallographic structure.

The appearance of the new positive peak at 0 eV when increasing the temperature has the consequence that the sign of the integrated signal at the L_{II} edge of Er in $ErFe_2$ changes between low and high temperatures. At low temperature, its sign is the same as the one observed in all the RE with $4f$ localized electrons, while at high temperature (above 200 K), it could be qualified as "correct," "correct" meaning it allows us to deduce the expected projection of $\langle S_z(5d)\rangle$ on the quantization axis. Remember that these measurements are done below the compensation temperature, and the integrated signal at the L_{III} edge does not change in that temperature range.

The difference in behavior of the XMCD spectra at the L_{II} and L_{III} edges of Er in Laves phases should allow us to conclude that the $5d_{3/2}$ subband is more affected by the presence of the $3d$ transition metal than the $5d_{5/2}$ subband. We should conclude that in Er compounds, the low part of the $5d$ band (which is more hybridized with the $3d$ electrons) is of $j=3/2$ character, while the top of the band has a more pronounced $j=5/2$ character. This could explain why the XMCD at the L_{II} edge is less intense than at the L_{III} edge, the low part of the $5d$ band being occupied by the $5d$ electrons. This could also explain why the $E2$ transitions at the L_{II} edge are (except in the case of compounds with Fe) absorbed by the $E1$ contribution, since the $E1$ transitions at the L_{II} edge arise at a lower energy compared to the L_{III} one. This hypothesis should be confirmed by density of states calculations.

TABLE II. Parameters used to calculate the so-called β-derivative. ΔE is the energy separating two absorption spectra modeling transitions towards majority and minority spin density of states (DOS) (the minority spin DOS corresponds to the measured spectrum and the majority spin DOS corresponds to the measured spectrum shifted towards low energy). The factor $(1-\beta)$ is applied to transitions towards minority states to simulate the different overlap between the wave functions of the $2p$ core hole and the $5d$ up and down spin direction.

L_{II}	$ErFe_2$	$ErCo_2$	$ErAl_2$	$Er_2(SO_4)_3,8H_20$
ΔE (eV)	0.02010	0.02605	0.02790	0.02410
$(1-\beta)$	1.00032	0.99960	0.99920	0.99870
L_{III}	$ErFe_2$	$ErCo_2$	$ErAl_2$	$Er_2(SO_4)_3,8H_20$
ΔE (eV)	0.0475	0.0480	0.0365	0.0194
$(1-\beta)$	0.9964	0.9965	0.9964	0.9964

IV. ANALYSIS OF MODELS AND APPLICABILITY

To account for both the sign of the $E1$-XMCD signal and the nonstatistical branching ratio observed in the presence of a $4f$ orbital momentum, two main models had been recently developed.[29–33] They *will be briefly summarized, applied to our experimental data, and discussed in Secs. IV A and IV B; we will also compare our results to the other experimental works applying these models. Reflections concerning the questions they still ask and the use of the sum rules will be proposed in Sec. IV C.*

A. Model proposed by van Veenendaal *et al.* (Refs. 29 and 30)

1. Description

The model proposed by van Veenendaal *et al.*[29,30] is derived from atomic calculations on ionic RE($5d^0$).[46] The shape of the signal is mainly determined by the interactions of the photoelectron with the open $4f$ shell, the spin and orbital parts of the Coulomb interaction being included. The spectra obtained present a dispersive line shape.[46] The authors validated their model with measurements on ionic systems done by Neumann *et al.*[34] Basing themselves on the observation that for RE in a metallic state, the spectra have a less dispersive line shape, van Veenendaal *et al.* suggest that the dissymmetry of the spectra comes from the metallic character of the RE and arises from the fact that the $5d$ orbitals contract or expand due to spin *and orbital* Coulomb interaction with the $4f$ electrons. The authors called it the breathing effect, leading to the enhancement of matrix elements (EME) and labeled β in that case.

In this atomic framework, the $5d$ orbitals with different radial extend are created by mixing them with different d orbitals. They are coupled together by the Coulomb spin and orbital interactions with the open $4f$ shells. The ground state is considered to have no d electron. In such a model, the integrated XMCD spectra at the $L_{II,III}$ edges of RE are found to be proportional to the ground-state expectation values of the magnetic operators in the $4f$ shell.[29] The evolution of integrated XMCD signals at each edge for the different RE (Ref. 29) reproduces the experimental ones.[11] The XMCD spectra have been simulated[30] using Cowan's programs.[47] The final state is a configuration interaction of $\underline{2p},4f^m,5d^1$ and $\underline{2p},4f^m,nd^1$, where the bar means a $2p$ core hole, m is the number of $4f$ electrons, and n is the main quantum number of the d shells ($n \geqslant 6$). The β parameter resulting from their calculation is equal to 0.24. The spectra display some interesting features (number of peaks, relative amplitudes) as compared to the experimental results. The absolute sign of the signals in Ref. 30 appears in agreement with the experimental one, even if the authors do not comment on that very important point. The scale of amplitudes is also not given, so it is not possible to quantitatively compare with the experimental effect. The authors point out that their theory cannot predict the fact that the XMCD spectra are more derivative-like when they are small. The authors also conclude that the presence of one $5d$ electron in the initial state should not change their results too much, since the ground-state expectation values of $5d$ operators are negligible as compared to the $4f$ ones.

2. Application and analysis

In an independent-particle picture, the derivative shape of the XMCD spectrum should arise from the difference of the two $5d$ spin subbands shifted by the magnetic exchange. The x-ray absorption spectrum is considered to represent the probed empty density of states ($5d$ in our case). Assuming a rigid band model, the two spin subbands are also represented by the same absorption spectrum; the derivative is then obtained by shifting them and subtracting them. A way to mimic the breathing effect (modification of the matrix elements) is to multiply one of these absorption spectra by a constant coefficient. This neglects the orbital dependence of the $4f$-$5d$ Coulomb interaction.

We calculated the derivative of the absorption spectra (what we called the β derivative) in order to compare it to our XMCD measurements. The β derivative is obtained by shifting the measured absorption of ΔE towards low energy, by multiplying the absorption at higher energy by (1-β). The values of β and ΔE (Table II) have been adjusted to reproduce the shape and the amplitude of the $E1$-XMCD spectrum *applying no additional scaling factor to the β derivative*. The results for $ErFe_2$, $ErCo_2$, $ErAl_2$, and $Er_2(SO_4)_3$, $8H_20$ are presented in Fig. 5.

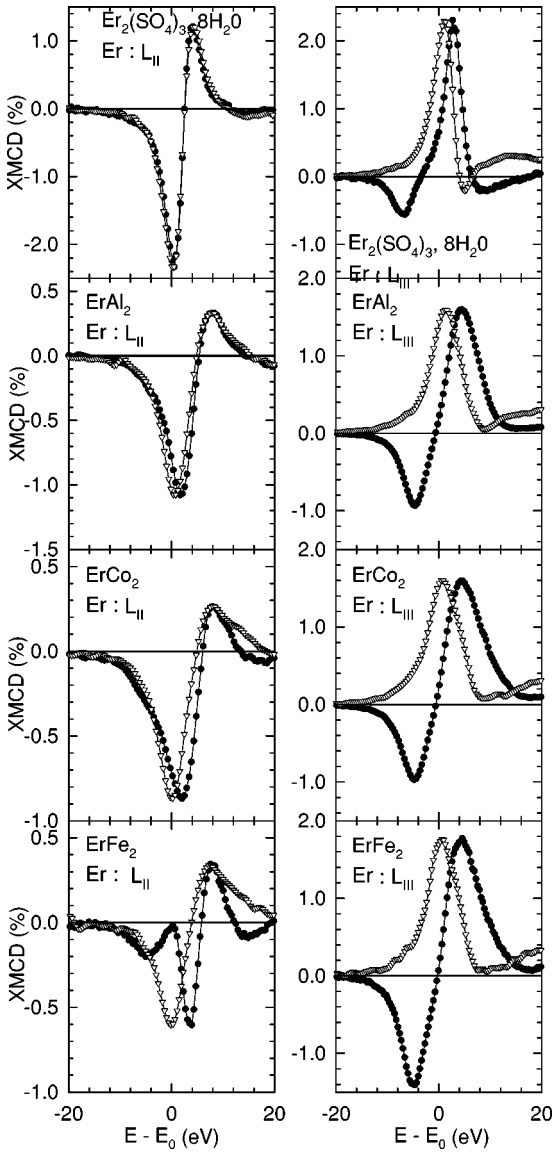

FIG. 5. Comparison between the XMCD spectra (black dots) and the β derivative of the absorption (white triangles).

At the L_{II} edge, the XMCD in the ionic compound can be exactly reproduced, but using a nonzero β coefficient. For the metallic compounds, *an energy shift between the β derivative and the XMCD appears*. In the case of $ErFe_2$, the width of the β derivative is very different from the $E1$-XMCD spectrum. *At the L_{III} edge, the XMCD spectra can never be reproduced by the β derivative of the absorption: the energy position is never correct*.

The values of the β coefficients are 10 to 100 times smaller than the XMCD effect. At the Er-L_{II} edge in $Erfe_2$, $(1\text{-}\beta)$ is greater than 1. The values of β do not have the same order of magnitude at the two edges, and are very different from the value of 0.24 resulting from the atomic calculation. The $4f$-$5d$ exchange can be evaluated to 0.5 eV. The ΔE values used in Table II are at least 10 times smaller. All the discrepancies cannot easily be justified.

Neumann *et al.*[34] have also compared their XMCD measurements at the $L_{II,III}$ edges of RE in ionic compounds to the derivative of the absorption spectra. They conclude that the spectra can be quite well modeled by a derivative of the absorption edge ($\beta=0$) at the L_{II} edge, but not at the L_{III} one. To explain the discrepancies, the authors invoked a crystal electric field (CEF) effect on the $5d$ states, which should affect quite severely the L_{III} edge but not the L_{II} one. Their spectra in Er_2O_3 (Ref. 34) are similar to our spectra in $Er_2(SO_4)_3$, $8H_20$. One can notice that they pointed the $E2$ contribution at the Er-L_{III} edge at -9.8 eV relative to the absorption maximum, which is in agreement with our value of 8353.5 ± 0.5 eV. More generally, the spectra in all the ionic systems are more or less similar (theirs and ours); at the L_{II} edge, they are not purely dispersive. We reproduce the XMCD at the Er-L_{II} edge in $Er_2(SO_4)_3$, $8H_20$ using the β-derivative model, but with a nonzero β coefficient. Nevertheless, the small value of β should be reasonable if we consider that Er in $Er_2(SO_4)_3$, $8H_20$ is not exactly a $5d^0$ state; but the XMCD at the L_{III} edge of Er in $Er_2(SO_4)_{3,}$, $8H_20$ cannot be reproduced.

For the metallic spectra, for which this model is devoted, neither at the L_{III} nor at the L_{II} edge can the XMCD spectra be reproduced: the energy position is always shifted. Moreover, the values of β and ΔE (Table II) for the metallic systems are of the same order of magnitude than the ones for the ionic compound. The CEF effects invoked by Neumann *et al.*[34] to justify the worse agreement at the L_{III} edge as compared to the L_{II} edge can perhaps be argued for the ionic compounds; they seem less justified for the metallic ones, where the CEF splitting is of the order of magnitude of the bandwidth (typically $2-5$ eV). Nevertheless, our results show that the energy shift of the β derivative occurs in the metallic systems, as well as in the ionic ones. This way of applying the hypotheses of van Veenendaal *et al.* is certainly too crude, but it appears sufficient to evidence some major discrepancies.

B. Model proposed by Matsuyama *et al.* (Refs. 31 and 32)

1. Description

The model proposed by H. Matsuyama *et al.*[31] derives from the one proposed by Jo and Imada.[48] The $5d$ band is described as the juxtaposition of 10 monoelectronic states characterized by their spin s_d and orbital m_d atomic quantum number. The ground state contains one $5d$ electron, whose spin and orbital moments are determined by the energy position of each $5d$ monoatomic state E_{m_d,s_d}. These energies are calculated by taking into account the spin s_f and orbital m_f quantum numbers of the $4f$ electrons with the expression given by Condon and Shortley.[49] The probabilities of transition are calculated using the Fermi golden rule in the $E1$ approximation with the atomic spherical harmonic functions. At this point, the model accounts for the variation of the integrated signals at the L_{II} and L_{III} edges, but with a sign opposite to the experimental data.[48]

To reverse the sign, Matsuyama *et al.*[31] proposed to enhance the matrix elements by multiplying each transition towards a (s_d, m_d) state by a spin- and orbital-dependent factor $(1-\alpha E_{m_d,s_d})>1$. With $\alpha=0.6$ Matsuyama *et al.*[31] reproduce rather well the general trends of variations of the integrated

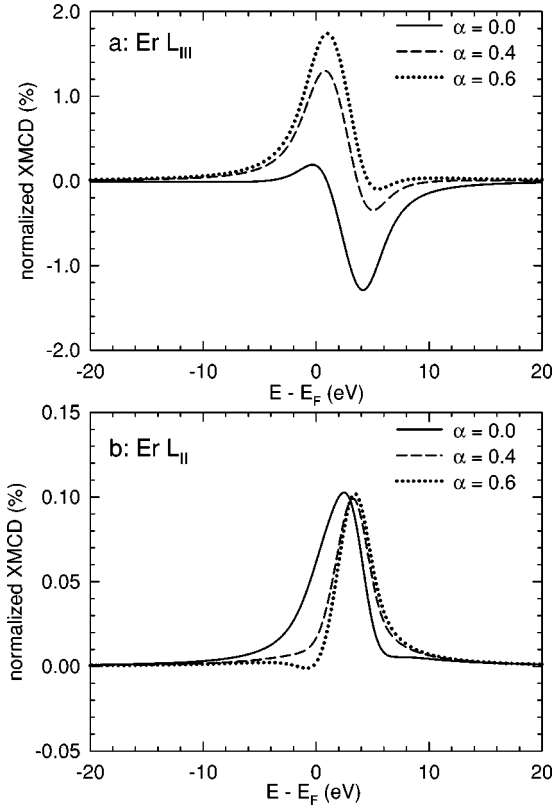

FIG. 6. Simulation of XMCD spectra at the (a) L_{III} and (b) L_{II} edges of Er using the model proposed by Matsuyama *et al.* (Ref. 31).

XMCD signals for all the RE with a sign in agreement with measurements. They also reproduced quite well the spectra at the $L_{II,III}$ edges of Pr as it is measured in Pr_2Co_{17} (Ref. 8) and in $Pr_2Fe_{17}B$,[35] but they have not published, to our knowledge, the spectra for the other RE with this model.

2. Simulation of Er spectra and analysis

We wrote a program[50] to simulate XMCD spectra with the model described above. The integrated XMCD spectra calculated with our program reproduced exactly Fig. 2 of Ref. 31 for all the RE.

The spectra for Er calculated with α equal to 0.0, 0.4, and $0.6(1/\mathrm{eV})$ are presented in Fig. 6. At the L_{III} edge [Fig. 6(a)], the spectrum is negative for $\alpha=0.0$, as expected from the projection of $\langle S_z(5d)\rangle$ on the quantization axis, but opposite to the measured $E1$ spectrum. The increase of α reversed the spectrum as expected from the model. For $\alpha=0.6$, the spectrum has an amplitude of 2% in agreement with the measured spectra in the metallic compounds. At the L_{II} edge [Fig. 6(b)], the spectra are composed of only one peak, whereas the measurements present two opposite structures. The calculated peak is always positive. Even for $\alpha=0.6(1/\mathrm{eV})$, the spectrum is not reversed. Such a result is in agreement with Fig. 2 of Ref. 31. In addition, the amplitude of the peak is more or less one order of magnitude smaller than our measurements. In conclusion, this model allows one to reproduce the features of the L_{III} edges of Er, but fails for the L_{II} edge.

One can notice that, since the maximum values of E_{m_d,s_d} are of the order of magnitude of 1 eV for all the RE, the term $-\alpha E_{m_d,s_d}$ calculated with $\alpha=0.6$ is around 0.6. This value has the same order of magnitude as the β coefficient calculated by van Veenendaal *et al.*[29,30] ($\beta=0.24$), which has the same physical origin, even if the way it is derived is different.

Based on the same kind of EME mechanism, but with a different description of the 5*d* band, the same authors' simulated the XMCD spectra of Nd^{3+} (Refs. 32 and 33) and Ho^{3+} (Ref. 33). They conclude that the competition between the enhancement effect and the filling of the low part of the 5*d* band is at the origin of the small signal observed at the L_{II} edge of heavy RE.[33] This is in agreement with our conclusion concerning the $j=\frac{3}{2}$ character of the low part of the 5*d* band in these systems.

A model derived from the one described in Sec. IV B 1 has also been applied by Fukui *et al.*[35] to simulate the XMCD spectra at the $L_{II,III}$ edges of RE in almost the entire series $RE_2Fe_{14}B$. They adapted the enhancement factor by scaling the E_{m_d,s_d} with a reduction factor R_E adjusted for each RE (it is equal to 0.15 for Er) and set α to $0.4(1/\mathrm{eV})$. This formalism allows the authors to calculate what they call the $E1$ part of the spectra resulting from the $4f$-$5d$ interaction. To account for the $3d$-$5d$ hybridization, the authors add to their calculated spectra the measured XMCD signals at the $L_{II,III}$ edge of La in $La_2Fe_{14}B$, or Lu in $Lu_2Fe_{14}B$, where the moment induced on the RE is purely due to the $3d$-$5d$ hybridization.

The general shape of the signals is reproduced, but the agreement between the simulations and the spectra is not perfectly achieved. The model fails in the case of the L_{II} edges of Tb, Dy, and Ho. For heavier RE($n_{4f}>10$), the XMCD signal at the L_{II} edge seems to be reproduced by the signal of La in $La_2Fe_{14}B$, or Lu in $Lu_2Fe_{14}B$, since the contribution calculated with the $5d$-$4f$ interaction is negligible compared to it. The XMCD spectra at the L_{III} edge of light RE, like Pr and Nd, present the same characteristics. One can wonder at the physical meaning of adding XMCD spectra due to different magnetic interactions to simulate the XMCD probing a band resulting from these different magnetic interactions. Actually, one should carefully study in which cases the spectra of Fukui *et al.*[35] really need the addition of the calculated and measured contributions to be reproduced. Indeed, it seems that in most of their measurements, either the spectra are dominated by the enhancement effect, and in these cases the signal of $La_2Fe_{14}B$ has an almost negligible influence, or the signal can be reproduced by the signal of $La_2Fe_{14}B$ or $Lu_2Fe_{14}B$ and the calculated spectrum resulting from the $4f$-$5d$ interactions does not change the shape significantly.

One has to notice that at the L_{II} edge of heavier RE($n_{4f}>10$), the sign of their measurement is "correct;" correct meaning that they give the expected $\langle S_z(5d)\rangle$ using the model of Schütz *et al.*[1] such as in $La_2Fe_{14}B$ or in $Lu_2Fe_{14}B$. This is not the case in our measurements at the L_{II} edge of Er in $ErFe_2$ at low temperature or in $ErCo_2$. Actually, our signals are also negative, but cannot be qualified as "correct." Indeed, for heavy RE, the projection of the RE sublattice magnetization on the quantization axis (given by the external

magnetic field) is opposite in $RE_2Fe_{14}B$ and in $REFe_2$ because of the ferrimagnetic alignment of RE and Fe sublattices magnetization, and the relative concentration of Fe and RE. That is why our spectrum at the L_{III} edge is opposite the one of $Er_2Fe_{14}B$. The sign of XMCD at the L_{II} edge of RE with $n_{4f}>10$ in the measurements of Fukui *et al.*[35] can perhaps be explained by the fact that they have been done at room temperature. The Curie temperatures of $RE_2Fe_{14}B$ are lower than 661 K,[51] thus the values of T/T_C for their measurements are around 0.5, and the signals could have evolved like in $ErFe_2$ at 300 K (Fig. 4). Another reason could be that the systems studied by Fukui *et al.*[35] have a higher concentration of Fe than ours, and our results show that this TM strongly modifies the spectrum at the L_{II} edge.

C. Remarks on these models and the sum rules

Up until now, the framework proposed by several groups to account for the sign of the $E1$ contribution is based on a "coefficient-derivative" model. The principle of a derivative model, based on the assumption that a rigid band model could be assumed, had been studied from the beginning of XMCD measurements at the $L_{II,III}$ edges of RE, when the whole XMCD spectra at the L_{III} edge of heavy RE were considered from the $E1$ origin. It had been abandoned because the sign of the derivative spectrum was opposite to the measured spectrum. When the $E2$ contribution was evidenced, it became clear that the $E1$ contribution was composed (at least mainly) of one positive peak in the case of the heavy RE. The derivative model was thus reconsidered, and the phenomenon invoked to transform the symmetric derivative into one peak was the filling of the $5d$ band. The result led to the wrong sign.

The phenomenon invoked now to transform the symmetric derivative into one peak with the sign of measurements is the enhancement of matrix elements, whose origin is the $4f$-$5d$ intra-atomic interaction. The deviation of the ratio of XMCD signals at the L_{II} and L_{III} edges of RE from the statistical value, linked to the application of the so-called $\langle L_z\rangle$ sum rule,[2,3] was interpreted by the existence of a $5d$ orbital momentum. The fact that this deviation appears as soon as the RE carries $4f$ orbital momentum led to the idea that the $5d$ orbital momentum should be induced by the $4f$ orbital momentum, with the consequence of taking into account the orbital component of the Coulomb interaction. But the application of the so-called $\langle S_z\rangle$ sum rule[4] to the same spectra gave the unexpected sign for $\langle S_z(5d)\rangle$, which leads to the EME mechanism. The question which arises naturally is the applicability of the $\langle L_z\rangle$ sum rule in the presence of EME.

The $\langle L_z\rangle$ sum rule is derived from absorption cross sections naturally described by the vacancy of each final state of the transition, multiplied by the corresponding $E1$ matrix elements, composed of radial and orbital parts, the orbital matrix element yielding to the projection of the orbital quantum number. In the models proposed to explain the XMCD at L edges of RE, the $E1$ matrix elements are modified by the EME, having the consequence that the projected orbital quantum numbers are no more multiplied by the population of the corresponding ground state: the sum rule thus has no reason to lead to $\langle L_z\rangle$. The same argument can be given for the $\langle S_z\rangle$ sum rule, the projection of the spin quantum numbers resulting from the spin-orbit coupling in the $2p$ core hole.

In the model proposed by Matsuyama *et al.*, where the ground state contains one $5d$ electron carrying a spin and orbital momentum, the impossibility of application of the sum rules can be easily derived from the expressions of the absorption. It can, of course, also be checked with the results obtained with the simulations: for Er, we calculated a value of $\langle L_z(5d)\rangle$ from the initial density of state equal to $-0.25\mu_B$/f.u.; the value calculated in applying the sum rule to the simulations with $\alpha=0.0$ is also $-0.25\ \mu_B$/f.u., while the value deduced from the application of the sum rule to the simulations with $\alpha=0.6$ is $+0.40\ \mu_B$/f.u.

In the model of van Veneendaal *et al.*, since the transitions are dominated by the interactions of the photoelectron with the $4f$ shell, the XMCD spectra lead to linear combinations of $\langle L_z\rangle$, $\langle T_z\rangle$, and $\langle S_z\rangle$ for the $4f$ shell and not the for the $5d$ one.

One can notice that the evolution of integrated XMCD spectra deduced from these models reproduces the experimental ones, which were correlated to the $4f$ magnetic properties. Such a conclusion is in favor of these models. Nevertheless, according to these models, the features of the spectra, and especially the deviation of the ratio of the intensities at the L_{II} and L_{III} edges from the statistical value, are no longer a proof of the presence of an orbital $5d$ momentum.

The so-called $\langle S_z\rangle$ sum rule[4] gives for $\langle S_z\rangle+(7/2)\langle T_z\rangle$ a sign which is opposite to the expected sign of $\langle S_z\rangle$. Because it has been admitted that $(7/2)\langle T_z\rangle$ should be smaller than $\langle S_z\rangle$, the sign of XMCD signals has been considered to be not "correct."

Recently, a simulation of XMCD spectra at the $L_{II,III}$ edge of Tb measured in a single crystal has been done in the framework of full multiple scattering theory,[52] using the FEFF8 code.[53] Without the use of EME, the sign of the signals appears to be the same as the measured one at both edges, even if that point is not underlined by the authors. The reason why the signal should be correctly reproduced, and thus why the XMCD could not account for the sign of $\langle S_z(5d)\rangle$, should come from the presence of the magnetic dipole operator $\langle T_z(5d)\rangle$.[54] This very important point should be confirmed, because the calculations done up to now by other authors in the framework of the full multiple scattering theory,[55] failed to reproduce the specific features of XMCD at the $L_{II,III}$ edges for the complete series of RE.

V. CONCLUSION

We measured XMCD spectra at the $L_{II,III}$ edges of Er in six samples exhibiting different kinds of $5d$ magnetization, going from the ionic state in $Er_2(SO_4)_3$, $8H_20$ to a metallic state with strong 5d-3d hybridization in $ErMn_2$, $ErFe_2$, $ErCo_2$, and $ErNi_2$, considering in between a metallic state with the $5d$ band hybridized with a nonmagnetic metal: Al.

Our experimental results show that the metallic compounds present features which are comparable to the ionic

compounds. This could confirm the fact that the intra-atomic $4f$-$5d$ interaction is a major point to explain the main characteristics of the spectra. But we also show the importance of the $3d$-$5d$ hybridization. Indeed, the difference observed at the L_{II} edge of Er in $ErFe_2$ and $ErCo_2$ cannot be explained by an atomic model. The Fe atoms induce an important modification of the $5d$ band, accompanied by a temperature dependence. Magnetostrictive effects do not seem to explain these phenomena.

This influence of the $3d$ transition metal is more visible at the L_{II} edge than at the L_{III} edge. This allows one to conclude that the low part of the $5d$ band has, in heavy RE, a $j=\frac{3}{2}$ character while the top of the band has a more pronounced $j=\frac{5}{2}$ character.

Our results also show that, except for $ErFe_2$, the $E1$ transition at the L_{II} edge of Er becomes so wide that it envelops the $E2$ contribution, explaining why it is so difficult to evidence it with the angular dependence of XMCD.

To explain the sign of the $E1$ contribution, two mains models have been proposed, based on the EME effect, but with different derivations and hypotheses. van Veenedaal *et al.* consider $5d^0$ systems, leading to derivative XMCD spectra, which are transformed into one peak due to the breathing effect of $5d$ orbitals resulting from the metallic character of the $5d$ band. Since the dominating effect is the interactions of the photoelectron with the open $4f$ shell, the presence of a $5d$ electron in the ground state is not important. Matsuyama *et al.* consider a $5d$ band with one electron in the ground state, leading to XMCD spectra composed of mainly one peak with the wrong sign, which is reversed due to an enhancement of matrix elements. These two models allow one to reproduce the main features of the integrated $L_{II,III}$ edges XMCD spectra: the sign of signals at both edges (due to EME) and the ratio of signals at both edges (due to the orbital component of the $4f$-$5d$ exchange Coulomb interaction). The general shape of the spectra is more or less reproduced. Nevertheless, a more quantitative comparison between spectra calculated by van Veenedaal *et al.* and experimental data should be interesting. The fact that XMCD spectra are more derivativelike when they are small cannot be predicted by the theory of van Veenendaal *et al.*, whereas it is explained by the presence of the $5d$ electron in the initial state by Matsuyama *et al.* The presence of a $5d$ electron in the ground state is the fundamental difference between these two kinds of models.

It results from this mechanism that the sum rules cannot be applied at the $L_{II,III}$ edges of RE, even the so-called $\langle L_z \rangle$ one.

The calculation done with the FEFF8 code, which seems to reproduce the XMCD spectra at the $L_{II,III}$ edges of Tb with the measured sign, without the use of EME, has to be confirmed on the other RE compounds.

To achieve a complete understanding of the XMCD spectra at the $L_{II,III}$ edges of RE in RE-transition-metal compounds, the $3d$-$5d$ hybridization should be included. It appears necessary to develop an *ab initio* calculation with an atomic description for the $4f$ states (LS coupling) and a band calculation for the $5d$ states, properly including the $4f$-$5d$ intra-atomic interaction and the $3d$-$5d$ hybridization.

ACKNOWLEDGMENTS

We acknowledge Christian Brouder for stimulating discussions on the different models and encouragements. We thank Valérie Paul-Boncour for useful discussions on $ErMn_2$ and on XMCD results on $ErFe_2D_x$ compounds. We thank all the technical groups from LURE who gave us support for maintenance and improvement of the experimental setup, and especially Laurent Pointal and Lucile Roussier from the Service Informatique et Expérience, Sébastien Chagnot and Jean-Michel Dubuisson from the Service Instrumentation de DCI, and Christian Pertel and Alain Jucha from the Service Electronique. We acknowledge Agnès Traverse for reading the manuscript and giving some helpful advice and encouragement.

[1] G. Schütz, W. Wagner, W. Wihlem, P. Kienle, R. Zeller, R. Frahm, and G. Materlik, Phys. Rev. Lett. **58**, 737 (1987).
[2] B. T. Thole, P. Carra, F. Sette, and G. van der Laan, Phys. Rev. Lett. **68**, 1943 (1992).
[3] M. Altarelli, Phys. Rev. B **47**, 597 (1993).
[4] P. Carra, B. T. Thole, M. Altarelli, and X. D. Wang, Phys. Rev. Lett. **70**, 694 (1993).
[5] M. Altarelli and Ph. Sainctavit, in *Magnetism and Synchrotron Radiation*, edited by E. Beaurepaire, B. Carrière, and J.-P. Kappler (Les Editions de Physique, Les Ulis, France, 1997), p. 65.
[6] D. Gignoux, in *Materials Science and Technology: Electronic and Magnetic Properties of Metals and Ceramics*, edited by K. H. J. Buschow (VCH, Weinheim, 1991), Vol. 3A.
[7] Peter Fischer, Ph.D. thesis, Fakultät für Physik der Technischen Universität München, Germany, 1993.
[8] P. Fischer, G. Schütz, S. Sthäler, and G. Wiesinger, J. Appl. Phys. **69**, 6144 (1991).
[9] F. Baudelet, Ch. Giorgetti, S. Pizzini, Ch. Brouder, E. Dartyge, A. Fontaine, J.-P. Kappler, and G. Krill, J. Electron Spectrosc. Relat. Phenom. **62**, 153 (1993).
[10] Ch. Giorgetti, S. Pizzini, E. Dartyge, F. Baudelet, Ch. Brouder, Ph. Bauer, G. Krill, S. Miraglia, D. Fruchart, and J.-P. Kappler, Phys. Rev. B **48**, 12732 (1993).
[11] Christine Giorgetti, Ph.D. thesis, LURE, Université Paris–Sud, Orsay, France, 1994.
[12] E. Dartyge, F. Baudelet, Ch. Giorgetti, and S. Odin, J. Alloys Compd. **275-277**, 526 (1998).
[13] P. Carra and M. Altarelli, Phys. Rev. Lett. **64**, 1286 (1990).
[14] G. Schütz, M. Knülle, R. Wienke, W. Wihlem, W. Wagner, P. Kienle, and R. Frahm, Z. Phys. B: Condens. Matter **73**, 67 (1988).
[15] P. Fischer, G. Schütz, S. Scherle, M. Knülle, S. Sthäler, and G. Wiesinger, Solid State Commun. **82**, 857 (1992).
[16] D. Gibbs, D. R. Harshman, E. D. Isaac, D. B. McWhan, D. Mills, and Ch. Vettier, Phys. Rev. Lett. **61**, 1241 (1988); J. P. Hannon, G. T. Trammel, M. Blume, and D. Gibbs, *ibid.* **61**, 1245 (1988).

[17] M. H. Krisch, C. C. Kao, F. Sette, W. A. Caliebe, K. Hämäläinen, and J. B. Hastings, Phys. Rev. Lett. **74**, 4931 (1995); F. Bartolomé, J.-M. Tonnerre, L. Sève, D. Raoux, J. Chaboy, L.-M. Garcia, M. H. Krisch, and C. C. Kao, *ibid.* **79**, 3775 (1997); F. Bartolomé, M. H. Krisch, D. Raoux, and J.-M. Tonnerre, Phys. Rev. B **60**, 13497 (1999).

[18] J. C. Lang, S. W. Kycia, X. D. Wang, B. N. Harmon, A. I. Goldman, D. J. Branagan, R. W. McCallum, and K. D. Finkelstein, Phys. Rev. B **46**, 5298 (1992); X. D. Wang, T. Leung, B. N. Harmon, and P. Carra, *ibid.* **47**, 9087 (1993); P. Carra, B. N. Harmon, B. T. Thole, M. Altarelli, and G. A. Sawatsky, Phys. Rev. Lett. **66**, 2495 (1991).

[19] J. C. Lang, G. Srajer, C. Detlefs, A. I. Goldman, H. König, X. D. Wang, B. N. Harmon, and R. W. McCallum, Phys. Rev. Lett. **74**, 4935 (1995).

[20] Ch. Giorgetti, E. Dartyge, Ch. Brouder, F. Baudelet, C. Meyer, S. Pizzini, A. Fontaine, and R.-M. Galéra, Phys. Rev. Lett. **75**, 3186 (1995).

[21] Ch. Giorgetti, E. Dartyge, F. Baudelet, and Ch. Brouder, Appl. Phys. A: Mater. Sci. Process. **73**, 703–706 (2001).

[22] J. Chaboy, F. Bartolomé, L.-M. Garcia, and G. Cibin, Phys. Rev. B **57**, R5598 (1998).

[23] U. Fano, Phys. Rev. **178**, 131 (1969).

[24] G. Schütz, P. Fischer, H. Ebert, R. Wienke, and W. Wilhelm, in *X-Ray Synchrotron Radiation Research*, edited by A. Balerna, E. Bernieri, and S. Mobilio (SIF, Bologna, Italy, 1990).

[25] Sylvie Odin, Ph.D. thesis, LURE, Université Paris–Sud, Orsay, France, 1998.

[26] S. Odin, F. Baudelet, E. Dartyge, J.-P. Itié, A. Polian, J.-C. Chervin, J. -P. Kappler, A. Fontaine, and S. Pizzini, Philos. Mag. B **80**, 155 (2000).

[27] R.-M. Galera, S. Pizzini, J. A. Blanco, J.-P. Rueff, A. Fontaine, Ch. Giorgetti, F. Baudelet, E. Dartyge, and M.-F. Lopez, Phys. Rev. B **51**, 15957 (1995).

[28] B. N. Harmon and A. J. Freeman, Phys. Rev. B **10**, 1979 (1974).

[29] M. van Veenedaal, J. B. Goedkoop, and B. T. Thole, Phys. Rev. Lett. **78**, 1162 (1997).

[30] M. van Veenedaal, J. B. Goedkoop, and B. T. Thole, J. Electron Spectrosc. Relat. Phenom. **86**, 151 (1997).

[31] H. Matsuyama, I. Harada, and A. Kotani, J. Phys. Soc. Jpn. **66**, 337 (1997).

[32] H. Matsuyama, K. Fukui, H. Maruyama, I. Harada, and A. Kotani, J. Magn. Magn. Mater. **177-181**, 1029 (1998).

[33] H. Matsuyama, K. Fukui, K. Okada, I. Harada, and A. Kotani, J. Electron Spectrosc. Relat. Phenom. **92**, 31 (1998).

[34] C. Neumann, B. W. Hooghenboom, A. Rogalev, and J. B. Goedkoop, Solid State Commun. **110**, 375 (1999).

[35] K. Fukui, H. Ogasawara, A. Kotani, I. Harada, H. Maruyama, N. Kawamura, K. Kobayshi, J. Chaboy, and A. Marcelli, Phys. Rev. B **64**, 104405 (2001).

[36] H. G. Purwins and A. Leson, Adv. Phys. **39**, 309 (1990).

[37] K. H. J. Buschow, Rep. Prog. Phys. **40**, 1179 (1977).

[38] J. X. Boucherle, A. Gregory, J. Schweizer, and G. Will, Physica B **156&157**, 734 (1989).

[39] F. Baudelet, E. Dartyge, G. Krill, J.-P. Kappler, Ch. Brouder, M. Piecuch, and A. Fontaine, Phys. Rev. B **43**, 5857 (1991); J.-P. Kappler, Ch. Brouder, G. Krill, F. Baudelet, E. Dartyge, A. Jucha, and A. Fontaine, in *X-Ray-Absorption Fine-Structure*, edited by S. Hasnain (Harwood, New York, 1991), p. 109; F. Baudelet, Ch. Brouder, E. Dartyge, A. Fontaine, J.-P. Kappler, and G. Krill, Europhys. Lett. **13**, 13751 (1990).

[40] H. Tolentino, E. Dartyge, A. Fontaine, and G. Tourillon, J. Appl. Crystallogr. **21**, 15 (1988).

[41] Carlos-Manuel Giles Antunez de Mayolo, Ph.D. thesis, Université Paris 7, France, 1995.

[42] Ch. Giorgetti, E. Dartyge, F. Baudelet, Ch. Brouder, and R.-M. Galéra (unpublished).

[43] E. Dartyge, F. Baudelet, Ch. Brouder, A. Fontaine, Ch. Giorgetti, J.-P. Kappler, G. Krill, M.-F. Lopez, and S. Pizzini, Physica B **208&209**, 751 (1995).

[44] V. Paul-Boncour (private communication).

[45] A. E. Clark, in *Ferromagnetic Materials*, edited by E. P. Wohlfarth (North-Holland, Amsterdam, 1980), Vol. 1, Chap. 7, p. 531.

[46] M. van Veenedaal, J. B. Goedkoop, and B. T. Thole (unpublished).

[47] R. D. Cowan, *The Theory of Atomic Structure and Spectra* (University of California Press, Berkeley, 1981).

[48] T. Jo and S. Imada, J. Phys. Soc. Jpn. **62**, 3721 (1993).

[49] E. U. Condon and G. H. Shortley, *The Theory of Atomic Spectra* (Cambridge University Press, Cambridge, England, 1959), Chap. VI, p. 159.

[50] Using the same notation as the Matsuyama *et al.*, we use the following formula:

$$I_{\pm}^{pj}(\hbar\omega) = \sum_{m_d,s_d,j_z} |M_{pjj_z,m_d,s_d}^{\pm}|^2 (1-\alpha E_{m_d,s_d}) \int_{E_F-E_{m_d,s_d}}^{W} d\varepsilon \times \rho_{m_d,s_d}(\varepsilon) L(\hbar\omega - E_{pj} - E_{m_d,s_d} - \varepsilon).$$

It is slightly different from the one cited by the authors since the formula proposed by the authors seems incorrect to us the shift of energy in the DOS has been omitted. All the parameters have been set to the same values. The energies of the states E_{m_d,s_d} have been calculated according to the expression given by Condon and Shortley Ref. 47, but the $c^k(lm_l, l'm_{l'})$ coefficients have been taken from the book of Condon and Odabasi [*Atomic Structure* (Cambridge University Press, Cambridge, England, 1980), p. 216], since the values of C^5 given on p. 178 of Ref. 47 are wrong. The values of Slater exchange integrals have been calculated using Cowan's program. For Er, we obtained $G^1 = 1.327$ eV, $G^3 = 1.061$ eV, and $G^5 = 0.804$ eV. These values are then scaled by a factor 0.8 to account for the solid state effects.

[51] J. F. Herbst, Rev. Mod. Phys. **63**, 819 (1991).

[52] H. Wende, Z. Li, A. Scherz, G. Ceballos, K. Baberschke, A. Ankudinov, J. Rehr, F. Wilhelm, A. Rogalev, D. L. Schlagel, and T. A. Lograsso, J. Appl. Phys. **91**, 7361 (2002).

[53] J. J. Rehr and A. Ankudinov, FEFF8, developed as "The FEFF Project," by the Department of Physics, University of Washington, Seattle, 1999.

[54] K. Baberschke (private communication).

[55] H. Ebert, Phys. Rev. B **38**, 9390 (1988); P. Strange, H. Ebert, J. B. Staunton, and B. L. Gyorffy, J. Phys.: Condens. Matter **1**, 2959 (1989); Ch. Brouder, M. Alouani, and K. H. Bennemann, Phys. Rev. B **54**, 7334 (1996).